

Smooth trajectory planning methods using physical limits

An Yong Lee¹ and Youngjin Choi²

Proc IMechE Part C:
J Mechanical Engineering Science
0(0) 1–17
© IMechE 2014
Reprints and permissions:
sagepub.co.uk/journalsPermissions.nav
DOI: 10.1177/0954406214553982
pic.sagepub.com



Abstract

In order for robots to be operated in a variety of environmental conditions, a smooth motion trajectory to goal point is needed in accordance with actuators specifications of the robot. In this paper, a conventional cubic polynomial method for symmetric curve (S-curve) trajectory planning is extended to the smooth (infinitely differentiable and continuous) symmetric and asymmetric curve (AS-curve) trajectory planning derived from a smooth jerk function. In other words, the proposed methods are able to generate the trajectory as S/AS-curve form as well as to satisfy several physical limits such as jerk limit, acceleration limit, and velocity limit. The effectiveness of the proposed methods is shown through comparative studies with existing method.

Keywords

Trajectory planning, smooth trajectory, symmetric curve, asymmetric curve

Date received: 8 April 2014; accepted: 8 September 2014

Introduction

Accompanied by the development of the computerized machines such as industrial robots and CNC (computer numerical control) machines, a fast and high precision motion control issue becomes more and more important. For the fast motion control, the inertias and masses of the moving parts in the computerized machine have been designed as light as possible, but it may cause the vibration problems due to the decrease of the structural stiffness. On the other hand, a smooth desired trajectory must be one of the important issues for the fast and high precision motion implementation. The smooth trajectory implies infinitely differentiable and continuous function, in short C^∞ function, in the paper. Most tasks of the industrial robots and CNC machines are given by either point-to-point moving or trajectory following, but this paper focuses on the trajectory tracking task of the robot and CNC control systems.

The smooth behavior of the robots and CNC machines improves a possibility for reducing the motion error that occurs while following the desired trajectory. When the fast and reliable motion is required for the computerized machines, higher-order (over third-order) polynomials are normally utilized, but they may yield a retrograde motion because they have large oscillations of the trajectories themselves.¹ Moreover, if the jerk (derivative of acceleration) is not limited within the actuator specification, it may cause the machines being damaged.^{1–3} It is also known that the jerk

minimization is required for the precise control performance such as a hard disk control.⁴ In addition, a residual vibration of the mechanical systems becomes one of the important issues for the control design as well as the desired trajectory planning. The trajectory planning considering the frequency response of the system was suggested in Biagiotti and Melchiorri.⁵ An objective function containing both terms proportional to the integral of the squared jerk and the total execution time was proposed in Gasparetto and Zanotto^{6–8} for the smooth trajectory. The higher-order polynomial functions have been utilized for the robotic manipulation in Boryga and Grabos.⁹ The optimal cubic-spline planning considering physical constraints was suggested in Rivera-Guillen et al.,¹⁰ Storey et al.,¹¹ and Ghasemi et al.¹² for the smooth trajectory. Moreover, a coordinate-free description for rigid body motion trajectories was suggested in De Schutter.¹³

On the other hand, since the industrial robots and the CNC machines require fast real-time control in low cost processors, the trajectory planning should be

¹Electrical, Electronic Control and Instrumentation Engineering, Hanyang University, South Korea

²Electronic Systems Engineering, Hanyang University, Ansan, South Korea

Corresponding author:

Youngjin Choi, Electronic Systems Engineering, Hanyang University, Ansan 426-791, South Korea.

Email: cyj@hanyang.ac.kr

simple algorithms for practical use as suggested in Ahn et al.¹⁴ and Macfarlane and Croft.¹⁵ Also, if we are to use the higher-order polynomials considering the actuator specifications simultaneously, then the computational complexity is greatly increased. As an alternative, cubic (third-order) symmetric curve (S-curve) trajectory planning has been used for motion profile instead of the higher-order polynomials. Advantages of the cubic S-curve trajectory planning are as follows; first it can be generated while satisfying the physical actuator specifications such as actuator's velocity and acceleration limits, second it can be realized with low computational cost.^{3,16–19}

Indeed, we have much more trajectory generation methods than the aforementioned, such as linear segment with parabolic blends (LSPB) and digital convolution-based method. The LSPB method in Costantinescu and Croft²⁰ and Bobrow et al.²¹ has been utilized for the desired trajectory generation, but it requires high computational effort in advance to match the blending points. The digital convolution-based method in Jeon and Ha²² and Lee et al.²³ must be efficient in a computational point of view, it may have a residual error at the final stage due to the discretization effect. Also, the digital convolution-based method was able to produce only symmetric trajectories.

The smooth symmetric curve (S-curve) trajectory planning method has been proposed in our previous paper.²⁴ In this paper, the smooth S-curve method is extended to the asymmetric curve (AS-curve) case of the velocity profile. When we use the asymmetric velocity profiles, the resulting motion is generated with different starting and approaching speeds. The basic idea of asymmetric curve velocity profiles has been suggested in Zou et al.²⁵ and Tsay and Lin,²⁶ but the jerk profile was not guaranteed to be continuous while switching between the maximum and the minimum. The paper is organized as follows: the conventional S-curve trajectory planning method is explained in the next section. The section following it presents the smooth S-curve and AS-curve trajectory planning methods by replacing the min/max jerk profile with the smooth jerk function. For this, several conditions to be satisfied are developed in terms of specific time intervals. And then the simulation and experiment are performed to show the effectiveness of the proposed method in a later section. And finally, conclusions are given in the last section.

Conventional S-Curve method using min/max jerk

The conventional cubic S-curve trajectory planning is first reviewed; here, two constant min/max values for the jerk are utilized to generate the trajectory, but the constant jerks make the acceleration not to be differentiable. This is one of the disadvantages of the conventional method. Here notice that two constant

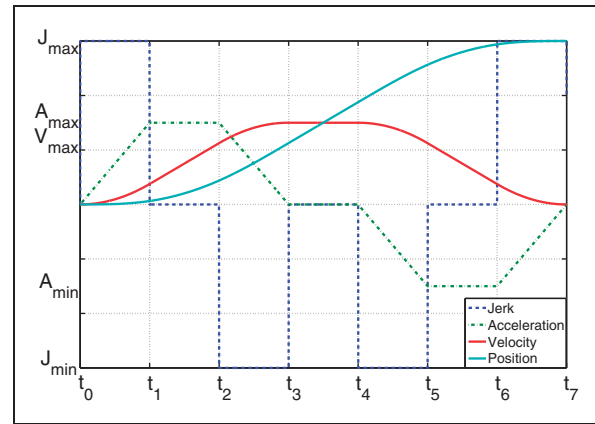


Figure 1. Jerk, acceleration, velocity, and position profiles by conventional cubic S-curve trajectory planning.

min/max jerks are normally given as opposite signs of the same magnitude. For given physical limits such as J_{\max} (jerk limit given as an actuator specification, note that $J_{\min} = -J_{\max}$), A_{\max} (acceleration limit, $A_{\min} = -A_{\max}$), and V_{\max} (velocity or speed limit), the cubic S-curve trajectory planning is illustrated in Figure 1. The constant jerk is integrated for the given time interval in order to obtain the trapezoidal acceleration profiles. Also, the acceleration and velocity profiles are sequentially integrated to obtain the velocity and position ones, respectively. From Figure 1, we can know that there are seven time intervals. Also notice that the profiles in the figure were obtained by applying all the zero initial/terminal conditions with respect to velocity, acceleration, and jerk. Now let us define the time intervals to be five independent variables as follows:

Time intervals: Descriptions

$$t_{j_a} = t_1 - t_0: \text{acceleration (constant jerk) time}$$

$$t_{a_a} = t_2 - t_1: \text{constant acceleration time}$$

$$t_{j_d} = t_3 - t_2: \text{acceleration (constant jerk) time}$$

$$t_{v} = t_4 - t_3: \text{zero acceleration (constant velocity) time}$$

$$t_{j_d} = t_5 - t_4: \text{deceleration (constant jerk) time}$$

$$t_{a_d} = t_6 - t_5: \text{constant deceleration time}$$

$$t_{j_d} = t_7 - t_6: \text{deceleration (constant jerk) time}$$

As shown in Figure 1, the conventional S-curve method generates the position profile from the rectangular jerk profiles by sequentially integrating them with the corresponding initial conditions. In the conventional method, since the acceleration time interval t_{j_a} is equal to the deceleration time interval t_{j_d} , the symmetric curve (S-curve) trajectory is generated as shown in Figure 1. In addition the constant acceleration time interval t_{a_a} becomes equal to the constant deceleration time interval t_{a_d} . Moreover, the conventional S-curve trajectory has the constant velocity time interval t_v in the mid of the generated trajectory

if the target distance is sufficiently large. Due to the symmetric property of the conventional S-curve method, seven time intervals (indeed, five independent variables) are reduced to three ones as follows:

$$\begin{aligned} t_j = t_{j_a} = t_{j_d}: & \text{ constant jerk time} \\ t_a = t_{a_a} = t_{a_d}: & \text{ constant acceleration time} \\ t_v: & \text{ constant velocity time} \end{aligned}$$

For each time interval, the S-curve trajectory is easily generated from the initial conditions of the corresponding time intervals as follows:

$$\begin{aligned} j(t) &= j(t_i^+) \\ a(t) &= j(t_i)(t - t_i) + a(t_i) \\ v(t) &= \frac{1}{2}j(t_i)(t - t_i)^2 + a(t_i)(t - t_i) + v(t_i) \\ x(t) &= \frac{1}{6}j(t_i)(t - t_i)^3 + \frac{1}{2}a(t_i)(t - t_i)^2 \\ &\quad + v(t_i)(t - t_i) + x(t_i) \end{aligned}$$

where $t_i \leq t \leq t_{i+1}$ for $i = 0, 1, \dots, 6$, and $j(t_i^+)$, $a(t_i)$, $v(t_i)$, and $x(t_i)$ represent initial conditions of jerk, acceleration, velocity, and position trajectory of each time interval, respectively. In particular, the initial/terminal conditions of piecewise continuous jerk functions have the following properties: $j(t_0^-) = 0$ and $j(t_0^+) = J_{\max}$ at $t = 0$, $j(t_1^-) = J_{\max}$ and $j(t_1^+) = 0$ at $t = t_1, \dots, j(t_6^-) = 0$ and $j(t_6^+) = J_{\max}$ at $t = t_6$. In addition, the initial conditions of acceleration segments should be within the actuator specifications as follows: $A_{\min} \leq a(t_i) \leq A_{\max}$ for each time interval of $i = 0, 1, \dots, 6$. In the case of the conventional S-curve method, the sum of all the time intervals is normally given by

$$t_{f,1} = 4t_j + 2t_a + t_v \quad (1)$$

Properties by actuator specifications

From the physical limits of the actuator, we can get a few properties with respect to the constant jerk and acceleration time parameters.

Property 1. For given actuator specifications, the constant jerk time is upper bounded by using the jerk and acceleration limits of the actuator as follows

$$t_j \leq \frac{A_{\max}}{J_{\max}} \quad (2)$$

where the equality is achieved if the jerk limit is constantly continued until the acceleration profile arrives at the acceleration limit.

In Property 1, the equality condition implies when the maximum duration of the constant jerk time is achieved. If the constant jerk time is determined beyond the inequality of equation (2), the trajectory is generated over the acceleration limit of the actuator. Hence, Property 1 should be always satisfied for the feasible trajectory.

Property 2. Assume that Property 1 is satisfied. If the trapezoidal acceleration profile is generated as shown in Figure 1, then the constant acceleration time is upper bounded by using the jerk, acceleration, and velocity limits of the actuator as follows

$$t_a \leq \frac{V_{\max}}{A_{\max}} - \frac{A_{\max}}{J_{\max}} \quad (3)$$

where the equality is achieved if the velocity profile arrives at the velocity limit at the time instant $t_3 = 2t_j + t_a$ in Figure 1.

The mathematical derivation of equation (3) is given in Appendix A1. In Property 2, the equality condition implies when the maximum duration of the constant acceleration time is achieved. However, as we can see in equation (3), non-positive value of t_a , namely $t_a \leq 0$, may appear according to the actuator specifications. It indeed implies that the constant acceleration time is not required for the feasible trajectory. As an alternative, the following property will be available for the feasible trajectory.

Property 3. If Property 2 fails to provide a positive $t_a > 0$, then the constant acceleration time duration as well as the acceleration limit are not required for the trajectory. In other words, since $t_a = 0$ and A_{\max} is not used for the trajectory, we again determine the inequality condition of the constant jerk time instead of Property 1 as follows

$$t_j \leq \sqrt{\frac{V_{\max}}{J_{\max}}} \quad (4)$$

where the equality is achieved if the velocity profile arrives at the velocity limit at the time instant $t_3 = 2t_j$ in Figure 1.

The mathematical derivation of equation (4) is given in Appendix A2. In Property 3, the equality condition implies when the maximum duration of the constant jerk time is achieved without making use of the acceleration limit of the actuator. For given actuator specifications such as J_{\max} , A_{\max} , and V_{\max} , we first check whether Property 2 is able to provide the feasible inequality condition or not. If it is available, Properties 1 and 2 are utilized to determine the time parameters according to the distance to be moved. Otherwise, Property 3 with $t_a = 0$ is utilized to determine the time parameter.

Distance criteria

Let us consider the case that Property 2 provides a feasible inequality condition. In this case, we have two distance criteria; the first distance criterion is defined as an unique distance that the velocity profile does arrive at the velocity limit V_{\max} as one point at the mid of the velocity profile as following form

$$S_1 = V_{\max} \left(\frac{A_{\max}}{J_{\max}} + \frac{V_{\max}}{A_{\max}} \right) \quad (5)$$

where the mathematical derivation is given in Appendix A3. The second distance criterion is defined as the unique distance that the acceleration profile does arrive at the acceleration limits A_{\max} and A_{\min} as two points at the time instants $t=t_j$ and $t=3t_j$ without using V_{\max} due to $t_v=0$ as follows

$$S_2 = 2A_{\max} \left(\frac{A_{\max}}{J_{\max}} \right)^2 \quad (6)$$

where the mathematical derivation is given in Appendix A4.

The third distance criterion is proposed for the case that Property 2 does not provide a feasible inequality condition. In the case, since $t_a=0$, the third criterion is obtained as the unique distance that the velocity profile does arrive at the velocity limit V_{\max} as one point at the mid of the velocity profile without using A_{\max} as follows

$$S_3 = 2V_{\max} \sqrt{\frac{V_{\max}}{J_{\max}}} \quad (7)$$

where the mathematical derivation is given in Appendix A5.

Time parameters determination by target distance

Now we are to present how to determine the constant jerk, acceleration, and velocity time parameters through the comparison between the proposed distance criteria and a target distance. The target distance S to be moved is defined as the difference between the initial position $x(t_0)$ and the terminal $x(t_f)$, namely, $S = |x(t_f) - x(t_0)|$, in which t_f and t_0 imply the terminal and initial time instant for the trajectory, respectively. Suppose that Property 2 provides a feasible inequality condition, then we have three cases classified by the first and second distance criteria.

Case I (when $S > S_1$): If the target distance is larger than the first distance criterion, then the constant jerk and acceleration time parameters are determined from the upper limits of equations (2) and (3), furthermore, the constant velocity time parameter

should be determined to accomplish the target distance as follows

$$t_v = \frac{S - S_1}{V_{\max}} \quad (8)$$

These results are summarized in the left column of Table 1.

Case II (when $S \leq S_1$ and $S > S_2$): If the target distance is not sufficiently large, namely $S \leq S_1$, then the constant velocity time period is not required, thus $t_v=0$. Also the target distance should be compared with the second distance criterion again. Here if $S > S_2$, then it implies the case when the constant acceleration time period is required to accomplish the target distance. In this case, the constant acceleration time parameter is determined with $t_v=0$ as follows

$$t_a = \sqrt{\frac{S}{A_{\max}} + \left(\frac{A_{\max}}{2J_{\max}} \right)^2} - \frac{3A_{\max}}{2J_{\max}} \quad (9)$$

where the mathematical derivation is given in Appendix A6. These results are summarized in the mid column of Table 1.

Case III (when $S \leq S_1$ and $S \leq S_2$): If the target distance is very small, namely $S \leq S_1$ and $S \leq S_2$, then both constant velocity and acceleration time periods are not required to accomplish the target distance, thus $t_v=0$ and $t_a=0$. Integrating rectangular jerk profiles three times becomes equal to the target distance as follows

$$S = 2J_{\max} t_j^3 \rightarrow t_j = \sqrt[3]{\frac{S}{2J_{\max}}} \quad (10)$$

The result is summarized in the right column of Table 1. On the other hand, suppose that Property 2 fails to provide a feasible inequality condition, namely $t_a=0$, then we have two cases classified by the third distance criterion.

Table 1. Three time parameters when Property 2 provides a feasible inequality condition, where S_1 and S_2 are the distance criteria defined by equations (5) and (6), respectively, and S is the target distance to be moved.

	$S \leq S_1$		
	$S > S_1$	$S > S_2$	$S \leq S_2$
t_j	$\frac{A_{\max}}{J_{\max}}$	$\frac{A_{\max}}{J_{\max}}$	$\sqrt[3]{\frac{S}{2J_{\max}}}$
t_a	$\frac{V_{\max}}{A_{\max}} - \frac{A_{\max}}{J_{\max}}$	$\sqrt{\frac{S}{A_{\max}} + \left(\frac{A_{\max}}{2J_{\max}} \right)^2} - \frac{3A_{\max}}{2J_{\max}}$	0
t_v	$\frac{S - S_1}{V_{\max}}$	0	0

Table 2. Three time parameters when Property 2 fails to provide a feasible inequality condition, namely when $t_a=0$, where S_3 is the distance criterion defined by equation (7).

	$S > S_3$	$S \leq S_3$
t_j	$\sqrt{\frac{V_{\max}}{J_{\max}}}$	$\sqrt[3]{\frac{S}{2J_{\max}}}$
t_a	0	0
t_v	$\frac{S - S_3}{V_{\max}}$	0

Case IV (when $S > S_3$): If the target distance is larger than the third criterion, then the constant jerk time parameter is determined from equation (4) and the constant velocity time parameter is determined according to the target distance as follows

$$t_v = \frac{S - S_3}{V_{\max}} \tag{11}$$

These results are summarized in the left column of Table 2.

Case V (when $S \leq S_3$): If the target distance is equal to or smaller than the third distance criterion, then the constant velocity time period is not required to achieve the target distance, thus $t_v=0$. Integrating the rectangular jerk profiles three times brings the condition of equation (10) again. The result is summarized in the right column of Table 2.

For the conventional S-curve method, how to determine the constant jerk, acceleration, and velocity time parameters according to the target distance has been suggested till now. However, when the min/max rectangular jerk functions are used, the generated trajectory does not have infinitely differentiable property. The next section will remedy it by introducing the smooth jerk profile.

Smooth trajectory planning

For smooth trajectory planning, we are first to introduce the smooth jerk function. Also, we will discuss about both advantages and disadvantages of the proposed method. Ultimately, the section proposes a smooth asymmetric-curve (in short, AS-curve) trajectory planning method.

Smooth jerk function

A smooth (infinitely differentiable and continuous) jerk function as a sinusoidal one is introduced as shown in Figure 2. Since the time integration of the sinusoidal function will often require integrating by part according to sequential integration from the jerk to the position. Thus, we will make use of the numerical (Euler) integration to get the acceleration,

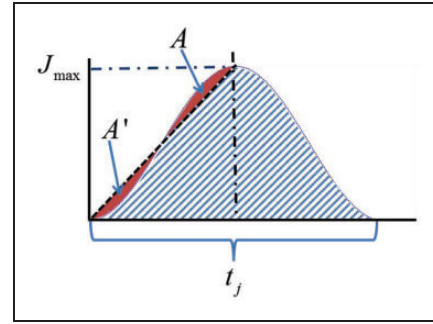


Figure 2. The shape of the proposed jerk function equation (12).

velocity, and position trajectories from the following discretized sinusoidal jerk function

$$j(n\Delta T) = J_{\max} \left(1 - \cos\left(\frac{2\pi}{t_j}(n\Delta T - t_i)\right) \right) \tag{12}$$

for $t_i < n\Delta T < t_{i+1}$ with $i=0, 6$, where ΔT implies the sampling time, t_j is the jerk time duration, n is the integer so that $n\Delta T=t$. For $i=2, 4$, J_{\max} of equation (12) is replaced with $J_{\min} = -J_{\max}$. Since the acceleration, velocity, and position profiles are obtained by the numerical integration, we have only to determine three time interval parameters such as t_j , t_a , and t_v , for smooth S-curve trajectory. Property 1 obtained from the rectangular jerk function should be modified because the sinusoidal jerk is utilized.

Property 1'. The shape of the jerk function of equation (12) is symmetric and the areas A and A' in the function must be equal to each other as shown in Figure 2. Hence, the jerk time parameter is upper bounded by using the jerk and acceleration limits of the actuator as follows

$$t_j \leq \frac{2A_{\max}}{J_{\max}} \tag{13}$$

where we should notice that $t_{j_a} = t_{j_d} = t_j$ for the S-curve trajectory and $t_{j_a} \neq t_{j_d}$ for the AS-curve trajectory.

Equation (13) in Property 1' is derived from the fact that the shaded area of Figure 2 should be equal to or smaller than the acceleration limit of the actuator, namely $\frac{1}{2}J_{\max} t_j \leq A_{\max}$. The jerk time duration of equation (13) becomes two times larger than that of equation (2). It would be the cost paid for the smooth trajectory. In the sequel, Properties 2 and 3 in the previous section will be also modified for the smooth trajectory.

Property 2'. For given acceleration profile obtained by integrating the proposed jerk functions, since the areas B and B' in Figure 3 are equal to each other, the

constant acceleration time is upper bounded as follows

$$t_a \leq \frac{V_{\max}}{A_{\max}} - \frac{2A_{\max}}{J_{\max}} \quad (14)$$

where we should also notice that $t_{a_a} = t_{a_d} = t_a$ for the S-curve trajectory and $t_{a_a} \neq t_{a_d}$ for the AS-curve trajectory.

Equation (14) is derived from the fact that the area of acceleration profile shown in Figure 3 should be equal to or smaller than the velocity limit of the actuator, in other words, it is obtained from $\frac{1}{2}A_{\max}t_j + A_{\max}t_a + \frac{1}{2}A_{\max}t_j \leq V_{\max}$ with the maximum jerk time duration $t_j = \frac{2A_{\max}}{J_{\max}}$. As we can see in equation (14), the inequality condition might be infeasible according to the actuator specifications such as $t_a \leq 0$. It implies that the constant acceleration trajectory duration is not required for the feasible trajectory. For the case of $t_a = 0$, we are to modify Property 3 as follows:

Property 3'. If equation (14) fails to provide the feasible condition, then the constant acceleration time duration is not required, namely $t_a = 0$. Also, since the A_{\max} is not utilized for the trajectory,

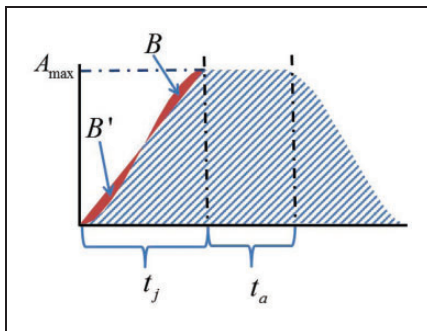


Figure 3. The shape of the acceleration profile obtained by using the proposed jerk functions.

we should determine again the jerk time parameter as follows

$$t_j \leq \sqrt{\frac{2V_{\max}}{J_{\max}}} \quad (15)$$

Equation (15) is derived from the fact that $\frac{1}{4}J_{\max}t_j^2 + \frac{1}{4}J_{\max}t_j^2 \leq V_{\max}$ due to $t_a = 0$.

Extensions to AS-curve

The modified properties in the previous section are extended to asymmetric curve (AS-curve) cases in this section. The AS-curve can be generated by using the different magnitude levels of jerk functions for acceleration and deceleration segments. For instance, the smooth AS-curve trajectory planning is illustrated in Figure 4, by using the given physical limits such as J_{acc} and A_{acc} for acceleration (in short, acc) segment, and J_{dec} and A_{dec} for deceleration (in short, dec) segment. Differently from the S-curve, we should consider five time intervals (t_{j_a} , t_{j_d} , t_{a_a} , t_{a_d} , t_v) for the AS-curve because $t_{j_a} \neq t_{j_d}$ and $t_{a_a} \neq t_{a_d}$. The jerk time parameters for acc/dec segments are obtained from the Property 1' as follows

$$t_{j_a} \leq \frac{2A_{acc}}{J_{acc}} \quad \text{and} \quad t_{j_d} \leq \frac{2A_{dec}}{J_{dec}} \quad (16)$$

Also we can get the constant acc/dec time parameters from Property 2' as follows

$$t_{a_a} \leq \frac{V_{\max}}{A_{acc}} - \frac{2A_{acc}}{J_{acc}} \quad \text{and} \quad t_{a_d} \leq \frac{V_{\max}}{A_{dec}} - \frac{2A_{dec}}{J_{dec}} \quad (17)$$

If equation (17) fails to provide the feasible conditions, namely $t_{a_a} \leq 0$ and $t_{a_d} \leq 0$, then both acceleration and deceleration limits, such as A_{acc} and A_{dec} , are not required for the trajectory planning. For the

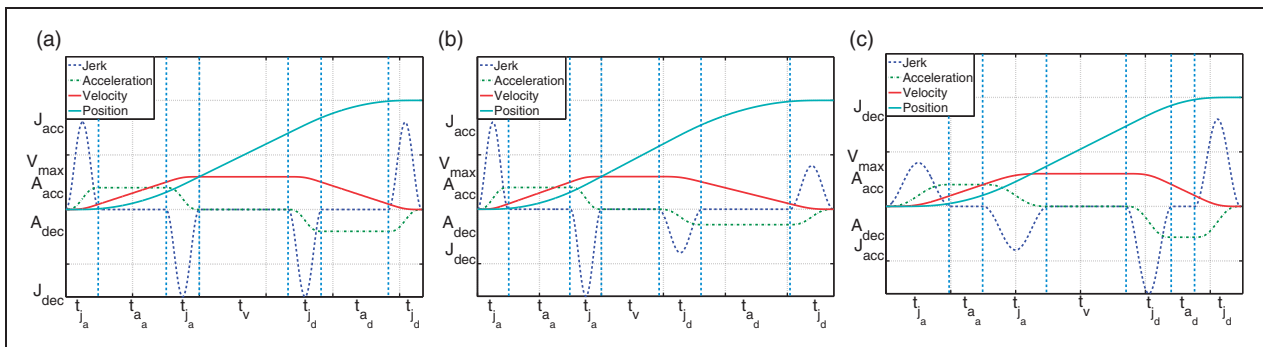


Figure 4. Jerk, acceleration, velocity, and position profiles by smooth S-curve and AS-curve trajectory planning: (a) S-curve when $J_{acc} = J_{dec}$ (or $k_r = 1$); (b) AS-curve when $J_{acc} > J_{dec}$ (or $k_r = \sqrt{2}$); (c) AS-curve when $J_{acc} < J_{dec}$ (or $k_r = 1/\sqrt{2}$).

case of $t_{a_a} = t_{a_d} = 0$, the jerk time parameters should be determined from Property 3' as follows

$$t_{j_a} \leq \sqrt{\frac{2V_{\max}}{J_{acc}}} \quad \text{and} \quad t_{j_d} \leq \sqrt{\frac{2V_{\max}}{J_{dec}}} \quad (18)$$

For simplicity, let us introduce the ratio parameter between acc and dec time segments as follows

$$t_{j_d} = k_r t_{j_a} \quad \text{and} \quad t_{a_d} = k_r t_{a_a}$$

where

$$k_r = \sqrt{\frac{J_{acc}}{J_{dec}}} = \frac{A_{acc}}{A_{dec}} \quad (19)$$

Also, we can easily confirm that the ratio satisfies equations (16), (17), and (18). However, if we use the ratio parameter of equation (19), it brings a constraint for physical limits to be satisfied. In other words, we have three independent parameters and one dependent parameter among J_{acc} , J_{dec} , A_{acc} , and A_{dec} . If we assign the jerk limit of the actuator to be J_{acc} , then J_{dec} would be determined by the ratio parameter and vice versa. Now we are to use the ratio of equation (19) for notational simplicity.

Figure 4 shows typical examples of smooth trajectory planning, in which Figure 4(a) is corresponding to the S-curve when $J_{acc} = J_{dec}$ (or $k_r = 1$), Figure 4(b) to the AS-curve when $J_{acc} > J_{dec}$ (or $k_r = \sqrt{2}$), and Figure 4(c) to the AS-curve when $J_{acc} < J_{dec}$ (or $k_r = 1/\sqrt{2}$). In the case of the AS-curve, the sum of all the time intervals is given by

$$\begin{aligned} t_{f,2} &= 2(t_{j_a} + t_{j_d}) + (t_{a_a} + t_{a_d}) + t_v \\ &= 2(1 + k_r)t_{j_a} + (1 + k_r)t_{a_a} + t_v \end{aligned} \quad (20)$$

Distance criteria for AS-curve

Now, we are to modify three distance criteria derived from the conventional S-curve method. If we can get positive t_{a_a} and t_{a_d} from equation (17) (derived from Property 2'), then we have two distance criteria. The first criterion S_1 determines whether the constant velocity duration is required or not, namely whether $t_v = 0$ or not, as follows

$$S_1 = \frac{V_{\max}}{2} \left(\frac{V_{\max}}{A_{acc}} + \frac{2A_{acc}}{J_{acc}} \right) + \frac{V_{\max}}{2} \left(\frac{V_{\max}}{A_{dec}} + \frac{2A_{dec}}{J_{dec}} \right) \quad (21)$$

where it implies the sum of two distances of acceleration and deceleration segments. Derivation of equation (21) is similar to Appendix A3.

The second criterion S_2 determines whether the constant acceleration and deceleration durations are

required or not, namely whether $t_{a_a} = t_{a_d} = 0$ or not, while $t_v = 0$, as follows

$$S_2 = A_{acc} \left(\frac{2A_{acc}}{J_{acc}} \right)^2 + A_{dec} \left(\frac{2A_{dec}}{J_{dec}} \right)^2 \quad (22)$$

where it implies the sum of two distances of acceleration and deceleration segments with $t_v = 0$. Derivation of equation (22) is similar to Appendix A4.

On the other hand, if equation (17) fails to provide the feasible inequality, then we set $t_{a_a} = t_{a_d} = 0$. Also, we need to check whether the constant velocity duration is required to accomplish the trajectory or not, namely whether $t_v = 0$ or not. Thus, we have introduced the third distance criterion as follows

$$S_3 = V_{\max} \left(\sqrt{\frac{2V_{\max}}{J_{acc}}} + \sqrt{\frac{2V_{\max}}{J_{dec}}} \right) \quad (23)$$

where it implies the sum of two distances of acceleration and deceleration segments with $t_{a_a} = t_{a_d} = 0$. Derivation of equation (23) is similar to Appendix A5.

Time parameters for smooth AS-curve method

Now, we are ready to present how to determine five constant time interval parameters through the comparison between the distance criteria (S_1 , S_2 , and S_3) proposed for the AS-curve and the target distance S . Suppose that equation (17) (derived from Property 2') provides the feasible inequality conditions, then we have three cases classified by the first and second distance criteria.

Case I (when $S > S_1$): If the target distance is larger than the first criterion S_1 of equation (21), then four time interval parameters are determined from the upper limits of equations (16), (17), and the ratio parameter of equation (19). And the remaining constant velocity time is determined according to the target distance as follows

$$t_v = \frac{S - S_1}{V_{\max}} \quad (24)$$

These results are summarized in the left column of Table 3.

Case II (when $S \leq S_1$ and $S > S_2$): If $S \leq S_1$ and $S > S_2$, then the trajectory does not arrive at the velocity limit, in other words, $t_v = 0$. After integrating acceleration profile two times, we get the following relation

$$\begin{aligned} S &= \frac{1}{2} A_{acc} (t_{a_a}^2 + 3t_{j_a} t_{a_a} + 2t_{j_a}^2) \\ &\quad + \frac{1}{2} A_{dec} (t_{a_d}^2 + 3t_{j_d} t_{a_d} + 2t_{j_d}^2) \end{aligned}$$

Table 3. Five time parameters when equation (17) (derived from Property 2') provides the feasible inequality condition, where S_1 and S_2 are the distance criteria defined by equations (21) and (22), respectively.

	$S \leq S_1$		$S \leq S_2$
	$S > S_1$	$S > S_2$	
t_{j_a}	$\frac{2A_{acc}}{J_{acc}}$	$\frac{2A_{acc}}{J_{acc}}$	$\sqrt[3]{\frac{2S}{J_{acc}(1+k_r)}}$
t_{j_d}	$k_r t_{j_a}$	$k_r t_{j_a}$	$k_r t_{j_a}$
t_{a_a}	$\frac{V_{max}}{A_{acc}} - \frac{2A_{acc}}{J_{acc}}$	$\sqrt{\frac{2S}{A_{acc}(1+k_r)} + \left(\frac{A_{acc}}{J_{acc}}\right)^2} - \frac{3A_{acc}}{J_{acc}}$	0
t_{a_d}	$k_r t_{a_a}$	$k_r t_{a_a}$	0
t_v	$\frac{S - S_1}{V_{max}}$	0	0

Now, if we apply the upper limits of equation (16) and the ratio parameter of equation (19) to above equation, we have

$$t_{a_a} = \sqrt{\frac{2S}{A_{acc}(1+k_r)} + \left(\frac{A_{acc}}{J_{acc}}\right)^2} - \frac{3A_{acc}}{J_{acc}}$$

$$t_{a_d} = k_r t_{a_a}$$

These results are summarized in the mid column of Table 3.

Case III (when $S \leq S_1$ and $S \leq S_2$): If $S \leq S_1$ and $S \leq S_2$, then the trajectory does not arrive at the physical limits of both velocity and accelerations, in other words, $t_v = 0$ and $t_{a_a} = t_{a_d} = 0$. After integrating jerk profile three times, we get the following relation

$$S = \frac{1}{2} \left(J_{acc} t_{j_a}^3 + J_{dec} t_{j_d}^3 \right)$$

Then by applying the upper limit of equation (16) and the ratio parameter of equation (19) to above equation, we have

$$t_{j_a} = \sqrt[3]{\frac{2S}{J_{acc}(1+k_r)}} \quad \text{and} \quad t_{j_d} = k_r t_{j_a} \quad (25)$$

These results are summarized in the right column of Table 3. On the other hand, suppose that equation (17) fails to provide the feasible inequality condition, then $t_{a_a} = t_{a_d} = 0$ and we have two more cases classified by the third distance criterion.

Case IV (when $S > S_3$): If $S > S_3$, then the jerk time durations are determined from upper limits of equation (18) and the remaining constant velocity time is determined according to the target distance as follows

$$t_v = \frac{S - S_3}{V_{max}} \quad (26)$$

Table 4. Five time parameters when equation (17) fails to provide the feasible inequality condition, namely when $t_{a_a} = t_{a_d} = 0$, where S_3 is the distance criterion defined by equation (23).

	$S > S_3$	$S \leq S_3$
	t_{j_a}	$\sqrt{\frac{2V_{max}}{J_{acc}}}$
t_{j_d}	$k_r t_{j_a}$	$k_r t_{j_a}$
t_{a_a}	0	0
t_{a_d}	0	0
t_v	$\frac{S - S_3}{V_{max}}$	0

These results are summarized in the left column of Table 4.

Case V (when $S \leq S_3$): If $S \leq S_3$, then the constant velocity time duration is not required to accomplish the target distance, namely $t_v = 0$. Integrating the jerk profiles three times brings the conditions of equation (25) again. These results are summarized in the right column of Table 4. Till now, we have completed the smooth AS-curve trajectory planning method. The next section will show the effectiveness of the proposed method through simulations and experiments.

Simulations and experiments

Application examples of the smooth S-curve and AS-curve methods are first suggested with physical limits of actuator, respectively. Also the comparative study with the conventional method is presented to mention both advantages and disadvantages of the proposed smooth methods. The experimental results are finally suggested for the verification of the practical use.

Example of smooth S-curve trajectory planning

Let us assume that we have an actuator with physical limits such as $J_{max} = 20 \text{ m/s}^3$, here $J_{max} = J_{acc} = J_{dec}$

for the S-curve, $A_{\max} = 3 \text{ m/s}^2$, here $A_{\max} = A_{\text{acc}} = A_{\text{dec}}$, and $V_{\max} = 2 \text{ m/s}$. Since the given actuator specifications provide the feasible inequality condition from equation (17), we can find the first and second distance criteria from equations (21) and (22), here, $S_1 = 1.933 \text{ m}$ and $S_2 = 0.540 \text{ m}$.

First let us assume that the target distance is $S = 5 \text{ m}$. Since the target distance is larger than the first criterion, $S > S_1$, we can find three nonzero time intervals t_j , here $t_j = t_{j_a} = t_{j_d}$ for the S-curve, t_a , here $t_a = t_{a_a} = t_{a_d}$, and t_v from Table 3. The resultant

plots are shown in Figure 5(a). Also, we can confirm from Figure 5(a) that all the profiles were generated by making active use of the physical actuator limits. Second, if we choose the target distance $S = 1.9 \text{ m}$, then it corresponds to the conditions $S \leq S_1$ and $S > S_2$ in Table 3. Accordingly, the time interval parameters are easily determined with $t_v = 0$. Also, we can confirm from Figure 5(b) that all the profiles were generated within the physical actuator limits without the constant velocity time duration. Third, if $S = 0.5 \text{ m}$, then it corresponds to

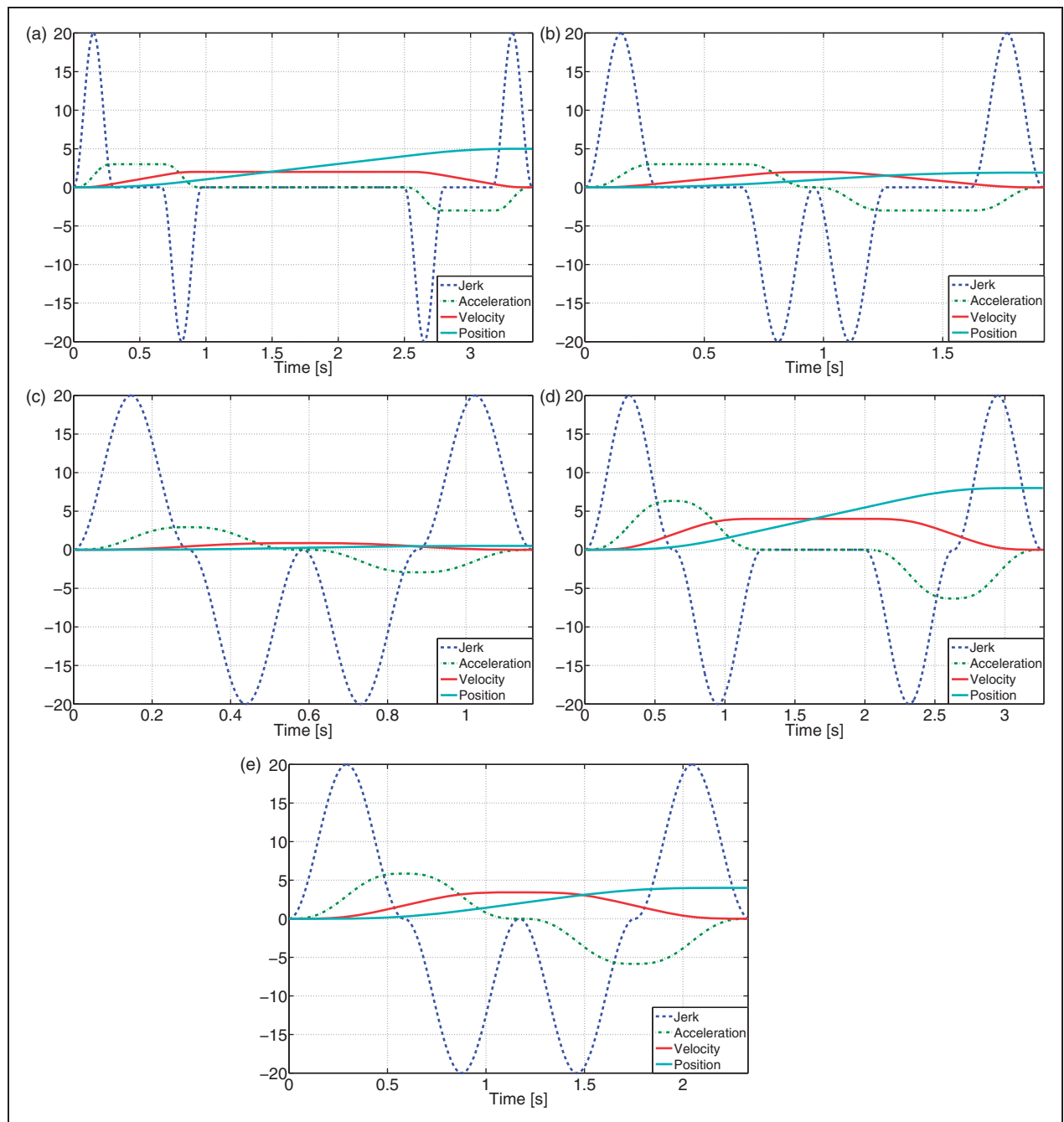


Figure 5. Simulation results for smooth S-curve corresponding to Cases I, II, III, IV, and V: (a) when $S > S_1$ (Case I); (b) when $S \leq S_1$ and $S > S_2$ (Case II); (c) when $S \leq S_1$ and $S \leq S_2$ (Case III); (d) when $S > S_3$ (Case IV); (e) when $S \leq S_3$ (Case V).

the conditions $S \leq S_1$ and $S \leq S_2$ in Table 3. Here, we can confirm from Figure 5(c) that all the profiles were generated within the physical actuator limits without the constant velocity and acceleration time durations.

On the other hand, assume that the physical limits are $J_{\max} = 20 \text{ m/s}^3$, $A_{\max} = 10 \text{ m/s}^2$, and $V_{\max} = 4 \text{ m/s}$. Then, since the given actuator specifications do not provide the feasible inequality condition from equation (17), we should find the third distance criterion from equation (23), here, $S_3 = 5.059 \text{ m}$. Fourth, if the target distance is given as $S = 8 \text{ m}$, then the time interval parameters are found from the condition $S > S_3$ in Table 4. Now, we can confirm from Figure 5(d) that all the profiles were generated within the physical actuator limits without the constant acceleration time duration. Fifth, if $S = 4 \text{ m}$, it corresponds to the condition $S \leq S_3$ in Table 4. Also, we can confirm from Figure 5(e) that all the profiles were generated within the physical actuator limits without the constant velocity and acceleration time durations.

Example of smooth AS-curve trajectory planning

For given physical limits of actuator such as $J_{\text{acc}} = 20 \text{ m/s}^3$, $J_{\text{dec}} = 10 \text{ m/s}^3$, $A_{\text{acc}} = 4 \text{ m/s}^2$, and $V_{\max} = 2 \text{ m/s}$, the ratio parameter is determined to be $k_r = \sqrt{2}$ from equation (19), and then $A_{\text{dec}} = 2.828 \text{ m/s}^2$ is accordingly determined from the ratio parameter k_r . Since the given actuator specifications provide the feasible inequality condition from equation (17), we can find both the first and second distance criteria as $S_1 = 2.172 \text{ m}$ and $S_2 = 1.545 \text{ m}$.

First, if $S = 8 \text{ m}$, then five nonzero time intervals are determined from the condition $S > S_1$ in Table 3. The resultant profiles are suggested in Figure 6(a). Second, if $S = 2 \text{ m}$, then it corresponds to the conditions $S \leq S_1$ and $S > S_2$ in Table 3. The generated profiles are shown in Figure 6(b). Third, if $S = 1.5 \text{ m}$, then it corresponds to the conditions $S \leq S_1$ and $S \leq S_2$ in Table 3. The result is shown in Figure 6(c).

On the other hand, let us assume that the physical limits of actuator are $J_{\text{acc}} = 20 \text{ m/s}^3$, $J_{\text{dec}} = 10 \text{ m/s}^3$, $A_{\text{acc}} = 7 \text{ m/s}^2$, and $V_{\max} = 4 \text{ m/s}$. With $k_r = \sqrt{2}$, we can find $A_{\text{dec}} = 4.949 \text{ m/s}^2$. Then, since the given actuator specifications do not provide the feasible inequality condition from equation (17), we should find the third distance criterion $S_3 = 6.107 \text{ m}$. Fourth, if $S = 8 \text{ m}$, then we can determine three nonzero time intervals from the condition $S > S_3$ in Table 4. The corresponding profiles are shown in Figure 6(d). Fifth, if $S = 4 \text{ m}$, then it corresponds to the condition $S \leq S_3$ in Table 4. The result is shown in Figure 6(e). From Figure 6, we can confirm that all the profiles were generated within the physical limits of the actuator while making active use of them.

Till now, we have shown the effectiveness of smooth S-curve and AS-curve trajectory planning methods through above two examples. The next section will suggest the comparison results between the conventional and the proposed smooth methods.

Comparative study with the conventional method

The conventional method suggested in the section ‘‘Conventional S-curve method using min/max jerk’’ and the proposed smooth S-curve planning method are compared to show the differences between them more clearly. When the target distance is given as $S = 5 \text{ m}$, if the physical limits are equal to the values ($J_{\max} = 20 \text{ m/s}^3$, $A_{\max} = 3 \text{ m/s}^2$, and $V_{\max} = 2 \text{ m/s}$) given in the first simulation of section ‘‘Example of smooth S-curve trajectory planning’’, then the phase portraits between the velocity and acceleration can be drawn as in Figure 7(a), here notice that the blue lines are differentiable but the red dotted line have four non-differentiable points in Figure 7(a). Also the terminal time of conventional S-curve method is $t_{f,1} = 3.317 \text{ s}$ from equation (1) and that of the proposed method is $t_{f,2} = 3.467 \text{ s}$ from equation (20). Since the proposed method makes use of the sinusoidal jerk functions, it takes a little bit more time to arrive at the target distance. Indeed, the time difference between them becomes

$$t_{f,2} - t_{f,1} = \frac{A_{\max}}{J_{\max}} \quad (27)$$

where we can confirm that the time difference of $t_{f,2} - t_{f,1} = 0.15 \text{ s}$ is exactly equal to $A_{\max}/J_{\max} = 3/20 = 0.15 \text{ s}$.

Now let us move to the AS-curve case. When the target distance is given as $S = 8 \text{ m}$, if the physical limits are equal to the values ($J_{\text{acc}} = 20 \text{ m/s}^3$, $J_{\text{dec}} = 10 \text{ m/s}^3$, $A_{\text{acc}} = 4 \text{ m/s}^2$, $A_{\text{dec}} = 2.828 \text{ m/s}^2$, $V_{\max} = 2 \text{ m/s}$) given in the first simulation of section ‘‘Example of smooth AS-curve trajectory planning’’, then we can confirm the smooth trajectory as shown in Figure 7(b). Here, notice that the red dotted lines have four non-differentiable points in Figure 7(b).

Aforementioned, the proposed method brings the smooth trajectory as an advantage, but it requires a little bit more time to arrive at the target distance as a disadvantage. As an alternative of the additional elapsed time, if it is possible to choose the peak value of the sinusoidal jerk function as twice maximum jerk of the conventional method, then we can make the terminal time of both methods to be the same values without changing the acceleration and velocity limits. For example, when the physical limits are given as $J_{\text{acc}} = 1.25 \text{ m/s}^3$, $J_{\text{dec}} = 0.625 \text{ m/s}^3$, $A_{\text{acc}} = 6.72 \text{ m/s}^2$, $A_{\text{dec}} = 4.75 \text{ m/s}^2$, and $V_{\max} = 2.5 \text{ m/s}$,

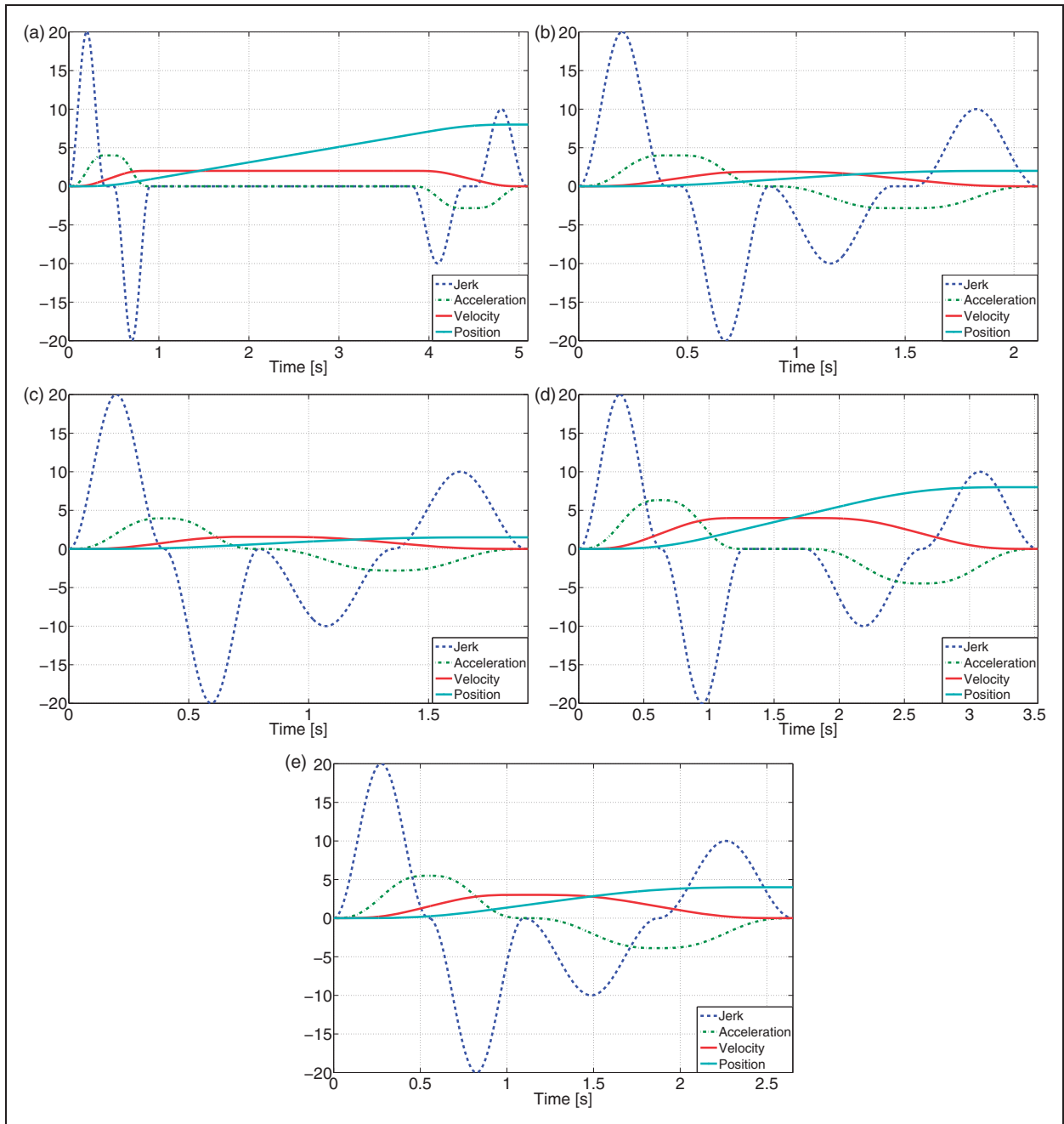


Figure 6. Simulation results for smooth AS-curve corresponding to Cases I, II, III, IV, and V: (a) when $S > S_1$ (Case I); (b) when $S \leq S_1$ and $S > S_2$ (Case II); (c) when $S \leq S_1$ and $S \leq S_2$ (Case III); (d) when $S > S_3$ (Case IV); (e) when $S \leq S_3$ (Case V).

if the peak values of the sinusoidal jerk functions can be chosen as $J_{acc_{peak}} = 2.5 \text{ m/s}^3 = 2J_{acc}$ and $J_{dec_{peak}} = 1.25 \text{ m/s}^3 = 2J_{dec}$, then both the conventional and the proposed methods make the trajectories to be terminated at the same time as shown in Figure 8.

Experimental results

The brushless EC-i40 (manufactured by Maxon Motor) DC motor is used for the experiment. According to the specifications of EC-i40, the nominal speed (maximum continuous speed) is

$8940 \text{ r/min} = 936.2 \text{ rad/s}$, the nominal torque (maximum continuous torque) is 0.0708 Nm and the rotor inertia is $2.43 \times 10^{-6} \text{ kg m}^2$. Now, let us determine the physical limits from above motor specifications as follows

$$\begin{aligned}
 V_{max} &= 936.2 \text{ rad/s} : \text{nominal speed} \\
 A_{acc} &= \frac{0.0708}{2.43 \times 10^{-6}} \\
 &= 29,135.8 \text{ rad/s}^2 : \frac{\text{nominal torque}}{\text{rotor inertia}}
 \end{aligned}$$

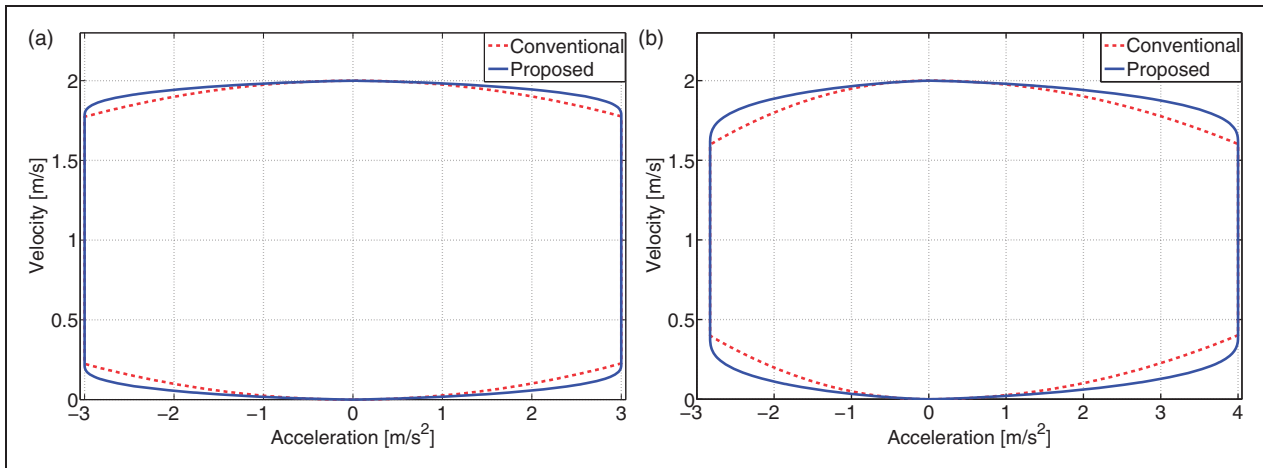


Figure 7. Phase portrait comparison between the conventional and the proposed methods: (a) S-curve planning; (b) AS-curve planning.

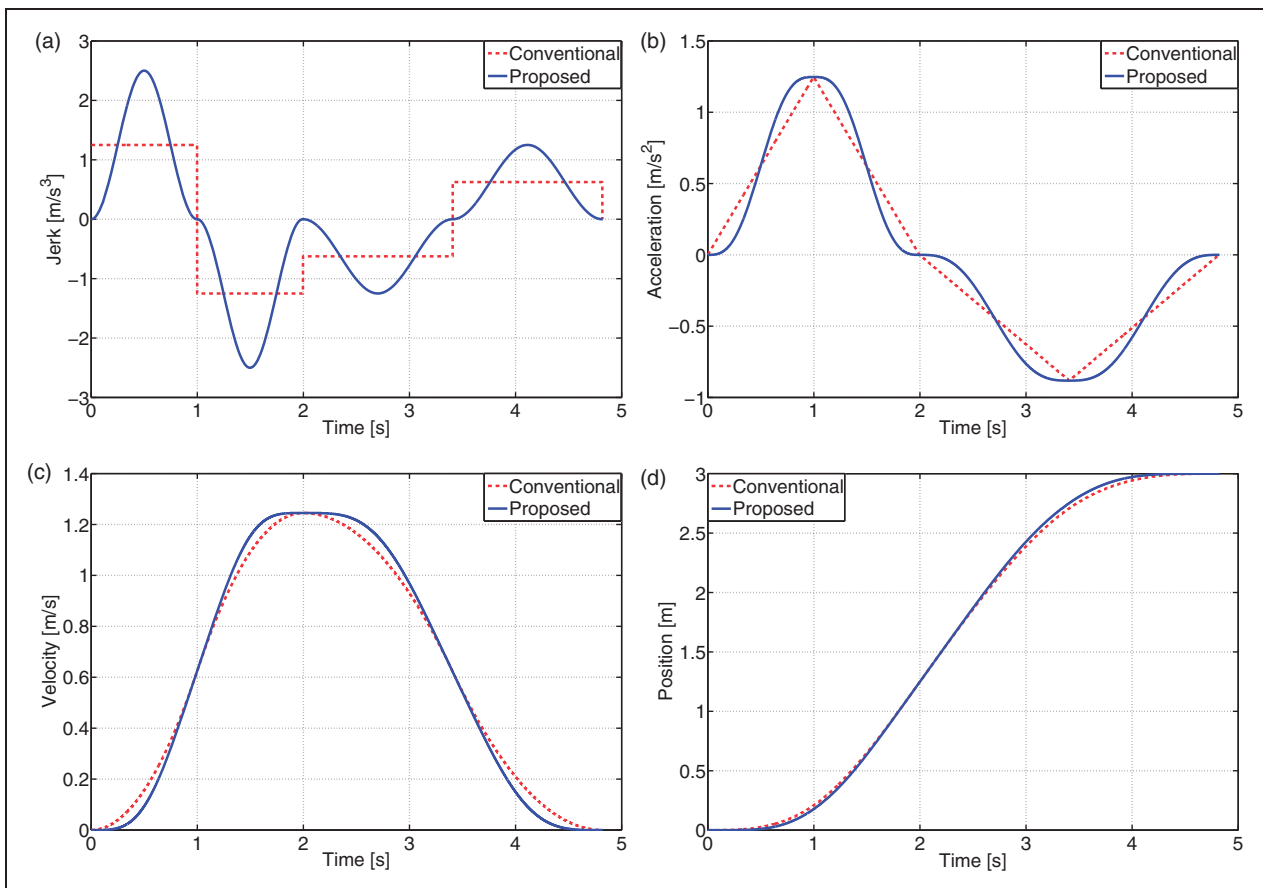


Figure 8. Performance comparisons between the conventional and the proposed methods when peak values of the sinusoidal jerk functions are twice max/min jerk values: (a) jerk profile; (b) acceleration profile; (c) velocity profile; (d) position profile.

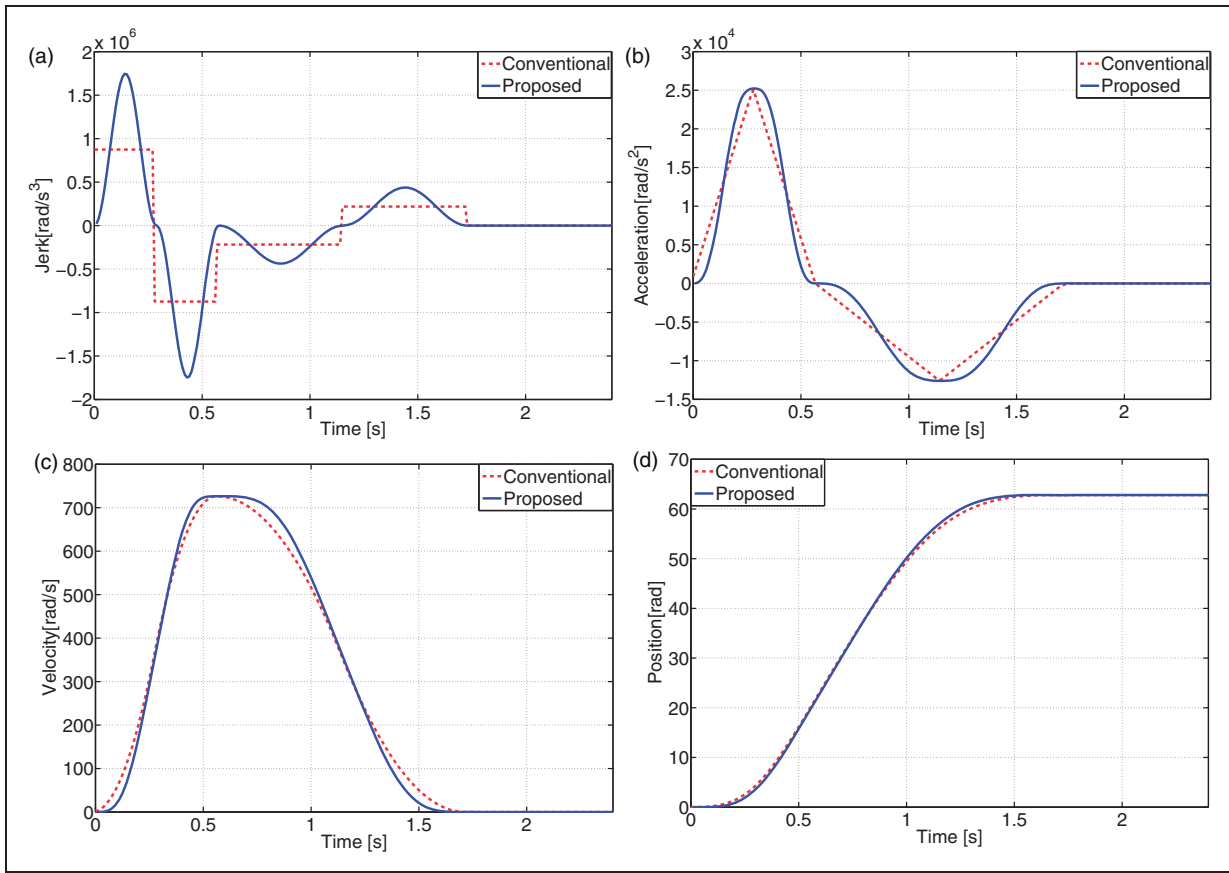


Figure 9. Desired profiles generated from the conventional and the proposed methods: (a) jerk profile; (b) acceleration profile; (c) velocity profile; (d) position profile.

Since the EC-i40 does not provide the data related to the jerk, we assume that the ratio between the jerk and acceleration is similar to the ratio between the acceleration and velocity (approximately 30 times). Then we have:

$$J_{acc} = 30 \times 29,135.8 = 874,074 \text{ rad/s}^3 : 30 \cdot A_{acc}$$

Also we assume that the deceleration is a half of the acceleration, namely $k_r = 2$. Now the remaining physical limits are determined as follows:

$$J_{dec} = 218,518.5 \text{ rad/s}^3 : J_{acc}/k_r^2$$

$$A_{dec} = 14,567.9 \text{ rad/s}^2 : A_{acc}/k_r$$

In addition, the peak values of sinusoidal jerk functions are determined as twice max/min jerks such as $J_{acc_{peak}} = 2J_{acc}$ and $J_{dec_{peak}} = 2J_{dec}$. Using above physical limits and the target distance $S = 62.8 \text{ rad}$, we are able to make the trajectories as shown in Figure 9 by using the conventional and the proposed methods. Notice that the generated trajectories are corresponding to the Case III ($t_v = 0$ and $t_a = t_d = 0$).

The controller for EC-i40 motor is chosen as the Elmo motor driver (solo whistle) with velocity mode. For given desired trajectories in Figure 9, the PI controller embedded in the Elmo motor driver is applied

in order to compare the performance difference between both methods. During the experiments, the velocity profiles were obtained as shown in Figure 10(a). Since the measured velocity profiles were noisy, the low-pass filter was applied and then we could get the filtered velocity profiles of Figure 10(b). Also we could confirm that the experimental velocity profiles suggested in Figure 10(b) are very similar to the desired velocity profiles of Figure 9(c). In addition, the velocity/position errors between the desired and actual (filtered) velocity/position were suggested in Figure 10(c) and (d). As we could see in Figure 10, the proposed smooth trajectory could bring a little bit smaller errors than the conventional method thanks to the smoothness of the generated trajectory. This would be another advantage of the proposed method.

Concluding remarks

The paper has proposed the smooth S-curve and AS-curve trajectory planning methods by using the sinusoidal jerk function. One of the big advantages of the proposed method brought the smooth profiles all the time, but it could be obtained at the cost of the additional elapsed time. As an alternative to the additional elapsed time, if it is possible to choose the

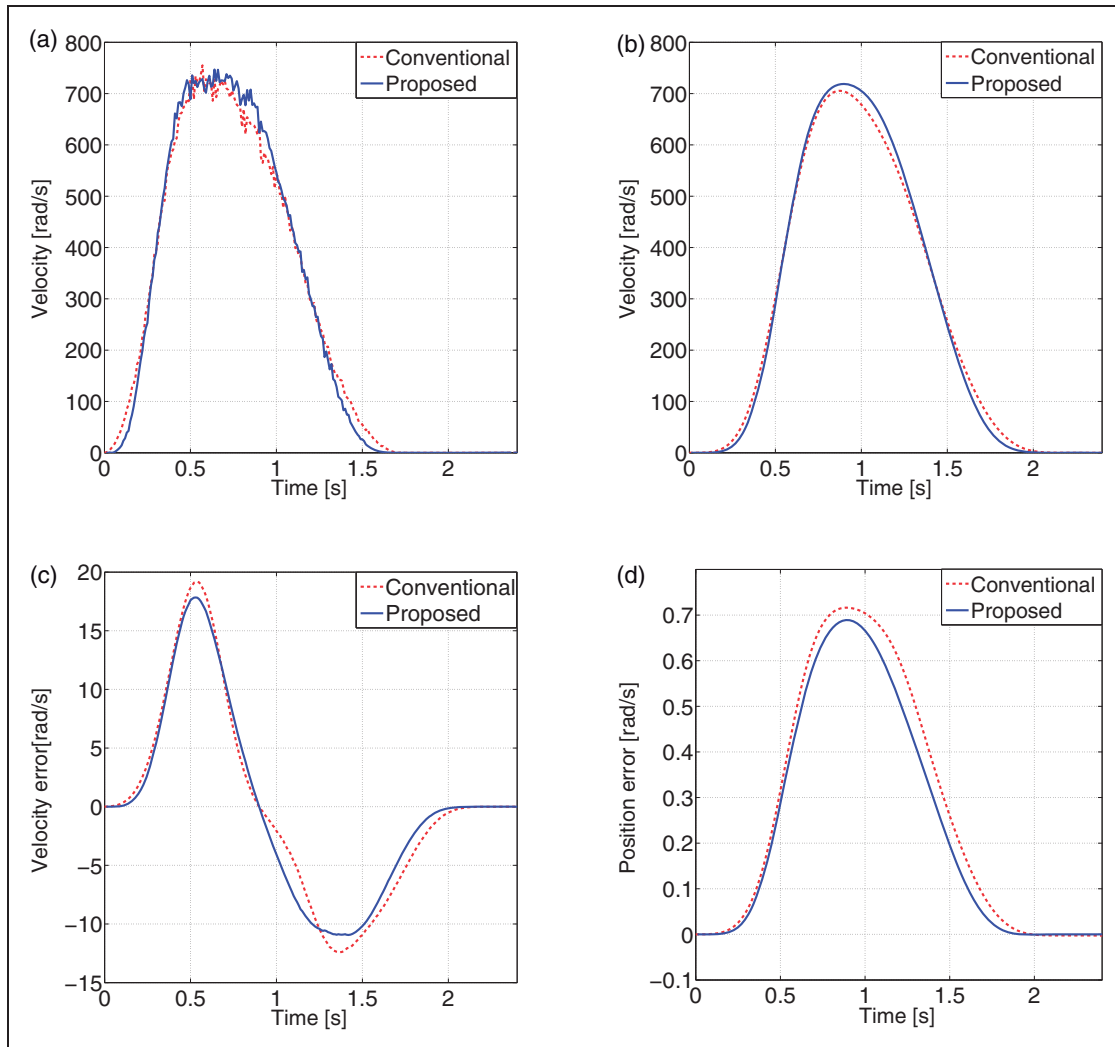


Figure 10. Experimental result: (a) measured raw velocity profiles; (b) low-pass filtered velocity profiles; (c) velocity error; (d) position error.

peak value of the smooth jerk function as twice maximum jerk for the conventional method, then we showed that the terminal time of both methods could be equal to each other. Moreover, all the profiles were obtained within the physical limits of the actuator by making active use of them. Also, we could confirm that the proposed smooth method brings better motion control performance. Finally, the effectiveness of the proposed method was presented through several simulations and experiments accompanied by comparative studies with the conventional method.

In future works, we are planning to apply the proposed method to the medical systems such as rehabilitation or wearable robots because it requires smooth jerk and acceleration behaviors for stable human-machine interactions.

Conflict of interest

None declared.

Funding

This work was supported in part by the Global Frontier R&D Program on “Human-centered Interaction for Coexistence” funded by the National Research Foundation of Korea grant funded by the Korean Government (MSIP) (NRF-2012M3A6A3057080), and in part by the National Research Foundation (NRF-2013R1A1A2010192), Republic of Korea.

References

1. Piazza A and Visioli A. Global minimum-jerk trajectory planning of robot manipulators. *IEEE Trans Ind Electron* 2000; 47(1): 140–149.
2. Gasparetto A, Lanzutti A, Vidoni R, et al. Validation of minimum time-jerk algorithms for trajectory planning of industrial robots. *J Mech Robot* 2011; 3(3): 031003.
3. Haschke R, Weitnauer E and Ritter H. On-line planning of time-optimal, jerk-limited trajectories. In: *IEEE/RSJ international conference on intelligent robots and systems*, Nice, France, 2008, pp.3248–3253.

4. Mizoshita Y, Hasegawa S and Takaishi K. Vibration minimized access control for disk drives. *IEEE Trans Magnet* 1996; 32(3): 1793–1798.
5. Biagiotti L and Melchiorri C. *Trajectory planning for automatic machines and robots*. New York: Springer, 2008.
6. Gasparetto A and Zanotto V. A new method for smooth trajectory planning of robot manipulators. *Mech Mach Theory* 2007; 42(4): 455–471.
7. Gasparetto A and Zanotto V. A technique for time-jerk optimal planning of robot trajectories. *Robot Comput-Integr Manuf* 2008; 24(3): 415–426.
8. Gasparetto A, Lanzutti A, Vidoni R, et al. Experimental validation and comparative analysis of optimal time-jerk algorithms for trajectory planning. *Robot Comput-Integr Manuf* 2012; 28(2): 164–181.
9. Boryga M and Grabos A. Planning of manipulator motion trajectory with higher-degree polynomials use. *Mech Mach Theory* 2009; 44(7): 1400–1419.
10. Rivera-Guillen J, Romero-Troncoso R, Osornio-Rios R, et al. Methodology for obtaining C3 continuity on tool trajectory featuring acceleration and jerk constraint on computer numerical control machine. *Proc IMechE, Part C: J Mechanical Engineering Science* 2011; 225(9): 2206–2215.
11. Storey I, Bourmistrova A and Subic A. Smooth control over jerk with displacement constraint. *Proc IMechE, Part C: J Mechanical Engineering Science* 2012; 226(11): 2656–2673.
12. Ghasemi M, Kashiri N and Dardel M. Time-optimal trajectory planning of robot manipulators in point-to-point motion using an indirect method. *Proc IMechE, Part C: J Mechanical Engineering Science* 2012; 226(2): 473–484.
13. De Schutter J. Invariant description of rigid body motion trajectories. *J Mech Robot* 2010; 2(1): 011004.
14. Ahn KT, Cho JS and Chung WK. Discrete trajectory formation in comparison with the analytical method for smooth movements. In: *Proceedings of IEEE conference on industrial electronics*, Paris, France, 2006, pp.4462–4467.
15. Macfarlane S and Croft EA. Jerk-bounded manipulator trajectory planning: Design for real-time applications. *IEEE Trans Robot Autom* 2003; 19(1): 42–52.
16. Broquere X, Sidobre D and Nguyen K. From motion planning to trajectory control with bounded jerk for service manipulator robots. In: *IEEE international conference on robotics and automation*, Anchorage, Alaska, USA, 2010, pp.4505–4510.
17. Broquere X, Sidobre D and Herrera-Aguilar I. Soft motion trajectory planner for service manipulator robot. In: *Proceedings of IEEE/RSJ international conference on intelligent robots and systems*, Nice, France, 2008, pp.2808–2813.
18. Nguyen KD, Ng TC and Chen IM. On algorithms for planning S-curve motion profiles. *Int J Adv Robot Syst* 2008; 5(1): 99–106.
19. Osornio-Rios RA, de Jesus Romero-Troncoso R, Herrera-Ruiz G, et al. FPGA implementation of higher degree polynomial acceleration profiles for peak jerk reduction in servomotors. *Robot Comput-Integr Manuf* 2009; 25(2): 379–392.
20. Costantinescu D and Croft E. Smooth and time-optimal trajectory planning for industrial manipulators along specified paths. *J Robot Syst* 2000; 17(5): 233–249.
21. Bobrow JE, Dubowsky S and Gibson J. Time-optimal control of robotic manipulators along specified paths. *Int J Robot Res* 1985; 4(3): 3–17.
22. Jeon JW and Ha YY. A generalized approach for the acceleration and deceleration of industrial robots and CNC machine tools. *IEEE Trans Ind Electron* 2000; 47(1): 133–139.
23. Lee G, Kim J and Choi Y. Convolution-based trajectory generation methods using physical system limits. *J Dyn Syst Meas Control* 2013; 135(1): 011001.
24. Lee AY, Jang G and Choi Y. Infinitely differentiable and continuous trajectory planning for mobile robot control. In: *The 10th international conference on ubiquitous robots and ambient intelligence*, Jeju, Korea, 2013, pp.357–361.
25. Zou F, Qu D, Wang J, et al. Asymmetric trajectory planning for vacuum robot motion. In: *IEEE international conference on robotics and automation*, Shanghai, China, 2011, pp.1–4.
26. Tsay DM and Lin CF. Asymmetrical inputs for minimizing residual response. In: *IEEE international conference on mechatronics*, Taipei, Taiwan, 2005, pp.235–240.

Appendix

Derivation of equation (3)

Assume that Property 1 is satisfied. If the trapezoidal acceleration profile is generated as shown in Figure 1, then the constant acceleration time is upper bounded by using the jerk, acceleration, and velocity limits of the actuator as follows

$$\frac{1}{2}A_{\max}t_j + A_{\max}t_a + \frac{1}{2}A_{\max}t_j \leq V_{\max} \quad (28)$$

$$t_j = \frac{A_{\max}}{J_{\max}} \quad \rightarrow \quad \therefore \quad t_a \leq \frac{V_{\max}}{A_{\max}} - \frac{A_{\max}}{J_{\max}}$$

where the equality is achieved when the velocity profile arrives at the velocity limit at the time instant $t_3 = 2t_j + t_a$ in Figure 1.

Derivation of equation (4)

Assume that Property 2 fails to provide the positive t_a . Then both the constant acceleration time period and the acceleration limit are not required for the trajectory. In other words, since $t_a = 0$ and A_{\max} is not used for the trajectory, we again determine the inequality condition of the constant jerk time instead of Property 1 as follows

$$\frac{1}{2}J_{\max}t_j^2 + \frac{1}{2}J_{\max}t_j^2 \leq V_{\max} \quad (29)$$

$$\therefore \quad t_j \leq \sqrt{\frac{V_{\max}}{J_{\max}}}$$

where the equality is achieved when the velocity profile arrives at the velocity limit at the time instant $t_3 = 2t_j$ in Figure 1. In other words, the equality condition implies when the maximum duration of the constant jerk time is utilized without making use of the acceleration limit of the actuator.

Derivation of equation (5)

The first distance criterion is defined as an unique distance that the velocity profile does arrive at the velocity limit V_{\max} as one point at the mid of the velocity profile as shown in Figure 11(a). As a mathematical form, the first distance criterion is defined by the area of velocity profile shown in Figure 11(a) as follows

$$\begin{aligned} S_1 &= 2 \left(\frac{1}{2} V_{\max} (t_j + t_a + t_j) \right) = V_{\max} (2t_j + t_a) \\ &= V_{\max} \left(\frac{A_{\max}}{J_{\max}} + \frac{V_{\max}}{A_{\max}} \right) \end{aligned} \quad (30)$$

where the upper limits of constant jerk and acceleration time parameters in Properties 1 and 2 were applied to the above equation.

Derivation of equation (6)

The second criterion is defined as the unique distance that the acceleration profile does arrive at the acceleration limits A_{\max} and $A_{\min} (= -A_{\max})$ as two points at the time instants $t = t_j$ and $t = 3t_j$, respectively, as shown in Figure 11(b) without using V_{\max} due to $t_v = 0$. The second distance criterion is obtained by integrating the acceleration profiles shown in Figure 11(b) twice as follows

$$\begin{aligned} S_2 &= 2 \left(\frac{1}{2} A_{\max} t_j^2 + \frac{1}{2} A_{\max} t_j^2 \right) = 2A_{\max} t_j^2 \\ &= 2A_{\max} \left(\frac{A_{\max}}{J_{\max}} \right)^2 \end{aligned} \quad (31)$$

where the upper limit of the constant jerk time parameter in Property 1 was applied to above equation.

Derivation of equation (7)

Since $t_a = 0$, the third distance criterion is obtained as the unique distance that the velocity profile does arrive at the velocity limit V_{\max} as one point at the mid of the velocity profile as shown in Figure 11(c) without using A_{\max} . The third distance criterion is defined by the area of the velocity profile shown in

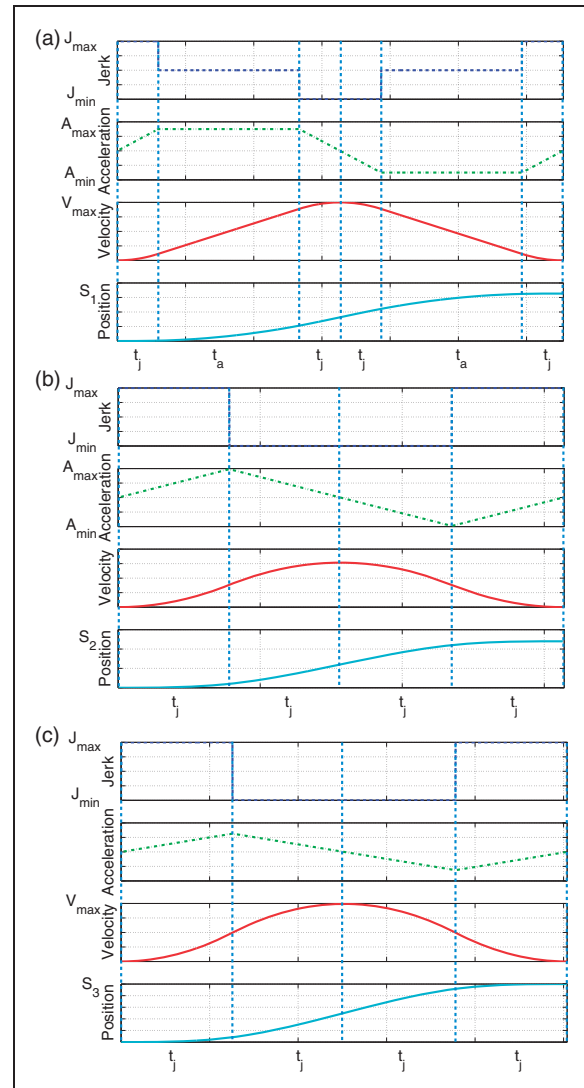


Figure 11. Distance criteria.

Figure 11(c) as follows

$$\begin{aligned} S_3 &= 2 \left(\frac{1}{2} V_{\max} (2t_j) \right) = V_{\max} (2t_j) \\ &= 2V_{\max} \sqrt{\frac{V_{\max}}{J_{\max}}} \end{aligned} \quad (32)$$

where the upper limit of the constant jerk time parameter in Property 3 was applied to above equation.

Derivation of equation (9)

When $S \leq S_1$ and $S > S_2$, if the target distance is not sufficiently large, then the constant velocity time period is not required, thus $t_v = 0$. Also, the target distance should be compared with the second distance criterion again. Here, if $S > S_2$, then it implies the case when the constant acceleration time period is

required to accomplish the target distance. After integrating the first trapezoidal acceleration profile, the maximum velocity of the trajectory is obtained as follows

$$v_{\max} = \frac{1}{2}A_{\max}t_j + A_{\max}t_a + \frac{1}{2}A_{\max}t_j = A_{\max}(t_j + t_a)$$

and we can get the following relation

$$\begin{aligned} S &= 2\left(\frac{1}{2}v_{\max}(2t_j + t_a)\right) \\ &= A_{\max}(2t_j^2 + 3t_jt_a + t_a^2) \end{aligned} \quad (33)$$

Now, if the upper limit of constant jerk time parameter of equation (2) is applied to the above equation, then the constant acceleration time parameter is determined as follows

$$\therefore t_a = \sqrt{\frac{S}{A_{\max}} + \left(\frac{A_{\max}}{2J_{\max}}\right)^2} - \frac{3A_{\max}}{2J_{\max}} \quad (34)$$